Published OnlineFirst October 26, 2017; DOI: 10.1158/1078-0432.CCR-17-2156

Biology of Human Tumors

Clinical Cancer Research

Low PD-1 Expression in Cytotoxic CD8$^+$ Tumor-Infiltrating Lymphocytes Confers an Immune-Privileged Tissue Microenvironment in NSCLC with a Prognostic and Predictive Value

Giulia Mazzaschi[1], Denise Madeddu[1], Angela Falco[1], Giovanni Bocchialini[2], Matteo Goldoni[3], Francesco Sogni[1], Giovanna Armani[1], Costanza Annamaria Lagrasta[4], Bruno Lorusso[4], Chiara Mangiaracina[4], Rocchina Vilella[1], Caterina Frati[1], Roberta Alfieri[5], Luca Ampollini[2], Michele Veneziani[6], Enrico Maria Silini[4], Andrea Ardizzoni[7], Konrad Urbanek[8], Franco Aversa[1], Federico Quaini[1], and Marcello Tiseo[6]

Abstract

Purpose: The success of immune checkpoint inhibitors strengthens the notion that tumor growth and regression are immune regulated. To determine whether distinct tissue immune microenvironments differentially affect clinical outcome in non–small cell lung cancer (NSCLC), an extended analysis of PD-L1 and tumor-infiltrating lymphocytes (TIL) was performed.

Experimental Design: Samples from resected adenocarcinoma (ADC 42), squamous cell carcinoma (SCC 58), and 26 advanced diseases (13 ADC and 13 SCC) treated with nivolumab were analyzed. PD-L1 expression and the incidence of CD3, CD8, CD4, PD-1, CD57, FOXP3, CD25, and Granzyme B TILs were immunohistochemically assessed.

Results: PD-L1 levels inversely correlated with N involvement, although they did not show a statistically significant prognostic value in resected patients. The incidence and phenotype of TILs differed in SCC versus ADC, in which *EGFR* and *KRAS* mutations conditioned a different frequency and tissue localization of lymphocytes. NSCLC resected patients with high CD8^{pos} lymphocytes lacking PD-1 inhibitory receptor had a longer overall survival (OS: HR = 2.268; 95% CI, 1.056–4.871, $P = 0.03$). PD-1-to-CD8 ratio resulted in a prognostic factor both on univariate (HR = 1.952; 95% CI, 1.34–3.12, $P = 0.001$) and multivariate (HR = 1.943; 95% CI, 1.38–2.86, $P = 0.009$) analysis. Moreover, low PD-1 incidence among CD8^{pos} cells was a distinctive feature of nivolumab-treated patients, showing clinical benefit with a prolonged progression-free survival (PFS: HR = 4.51; 95% CI, 1.45–13.94, $P = 0.004$).

Conclusions: In the presence of intrinsic variability in PD-L1 expression, the reservoir of PD-1–negative effector T lymphocytes provides an immune-privileged microenvironment with a positive impact on survival of patients with resected disease and response to immunotherapy in advanced NSCLC. *Clin Cancer Res; 24(2); 407–19. ©2017 AACR.*

Introduction

The central role of the immune system in the control of tumor growth and progression has been repeatedly demonstrated (1, 2). Accordingly, recently introduced molecules targeting immune checkpoints have received ground-breaking achievements in the treatment of several solid tumors, including non–small cell lung cancer (NSCLC; refs. 3–6). At variance with therapeutic approaches directed against neoplastic cells, such as chemotherapy or small molecule tyrosine kinase inhibitors (7, 8), targeting the interactions between programmed cell death-1 (PD-1), a T-cell coinhibitory receptor, and one of its ligands, programmed cell death-ligand 1 (PD-L1), has shown unprecedented success (9, 10).

Although the expression of PD-L1 by tumor cells potentially identifies NSCLC patients who would benefit from immune checkpoint inhibitors (ICI), it does not consistently represent a reproducible predictive biomarker of the clinical response (11–13). The attempt to correlate PD-L1 expression and patient prognosis has shown conflicting results (14–16). Extensively debated issues on antibody specificity and different methodologies (17, 18) have been partially overcome by several initiatives of harmonization (19–21). However, the variability of PD-L1 expression among and within NSCLC (17) is intrinsic to several biologic and genetic events implicated in tumor immunogenic properties (4, 14). In this regard, neoantigens generation (22, 23) and timing of the natural immune history largely vary among patients and markedly impact on PD-L1 expression.

[1]Hematology and Bone Marrow Transplantation, University Hospital of Parma, Parma, Italy. [2]Thoracic Surgery, University Hospital of Parma, Parma, Italy. [3]Medical Statistics, University Hospital of Parma, Parma, Italy. [4]Pathology, University Hospital of Parma, Parma, Italy. [5]Experimental Oncology, University Hospital of Parma, Parma, Italy. [6]Medical Oncology- Department of Medicine and Surgery, University Hospital of Parma, Parma, Italy. [7]Division of Medical Oncology, Sant'Orsola-Malpighi University Hospital, Bologna, Italy. [8]Department of Experimental Medicine, Section of Pharmacology, University of Campania "Luigi Vanvitelli," Naples, Italy.

Note: Supplementary data for this article are available at Clinical Cancer Research Online (http://clincancerres.aacrjournals.org/).

G. Mazzaschi and D. Madeddu contributed equally to this article.

Corresponding Author: Federico Quaini, Hematology and Bone Marrow Transplantation, University of Parma, via Gramsci 14, 43126 Parma, Italy. Phone: 390521033297; E-mail: federico.quaini@unipr.it

doi: 10.1158/1078-0432.CCR-17-2156

Published OnlineFirst October 26, 2017; DOI: 10.1158/1078-0432.CCR-17-2156

Translational Relevance

The wave of enthusiasm brought about by the success of PD-1/PD-L1 immune checkpoint inhibitors (ICI) in NSCLC points toward the emerging need to determine the clinical impact of distinct immune microenvironments. Tumor-infiltrating lymphocytes (TIL) critically contribute to tumor biology and response to ICI. Thus, in addition to the evaluation of PD-L1, predictive biomarkers likely require the simultaneous assessment of phenotypes relevant to PD-1/PD-L1 immune checkpoint. The inhibitory receptor PD-1, being also a therapeutic target, was a candidate to provide significant insights in NSCLC immune landscape and response to immunotherapy. Our data suggest that, in the presence of a variable degree of PD-L1 expression, an intrinsic reduction of PD-1^{pos} TILs is associated with delayed NSCLC progression, improved OS, and response to ICI. Based on our findings, the population of cancer patients who benefit from actual and innovative immunotherapeutic approaches may be expanded following a detailed characterization of the tumor immune microenvironment.

In addition, other components of the tumor microenvironment, such as tumor-infiltrating lymphocytes (TIL), critically contribute to tumor biology and therapeutic response to ICI (24), suggesting that predictive biomarkers aimed at personalized therapy can be obtained by a coordinated multiparametric definition of the immune contexture (24–27).

Specifically, the balance between PD-L1–mediated tumor immune escape and the efficient immune reaction against cancer by TILs may provide more relevant prognostic and therapeutic tools.

According to PD-L1 status and number of TILs, a classification of tumors into four categories has been recently proposed (28, 29). This includes type I adaptive immune resistance (PD-L1 positive and high TILs), type II immune ignorance (PD-L1 negative and low TILs), type III intrinsic induction (PD-L1 positive and low TILs), and type IV immune tolerance (PD-L1 negative and high TILs). However, a detailed tissue characterization of these different aspects of the immune mediated tumor growth and regression has been only partially investigated in NSCLC.

The present work was addressed to determine whether immunologically defined NSCLC tissue microenvironments might influence the clinical outcome and response to ICI. Thus, 100 newly diagnosed and surgically removed tumors and 26 samples from patients with advanced NSCLC candidate to receive anti–PD-1 drug (nivolumab) were morphometrically analyzed to assess the number and distribution of TILs subpopulations together with the immunohistochemical evaluation of PD-L1 expression. The hypothesis was advanced on whether and to which extent the expression of PD-1 inhibitory receptor on immune relevant cells exerts a prognostic and predictive effect. Thus, the potential association with clinical data of individual and integrated tissue parameters involved in PD-1/PD-L1 immune checkpoint was investigated in both groups of patients.

Materials and Methods

Patient population and tissue sampling

This study involved 100 NSCLC patients (58 SCC and 42 ADC, stage I/II 72%) undergoing lung resections with curative intent at the Unit of Thoracic Surgery, University-Hospital of Parma, and 26 patients (13 ADC and 13 SCC) with stage IIIb to IV treated with nivolumab in second or third-line therapy. The investigation was approved by the institutional review board for human studies (Ethical Committee) of the University-Hospital of Parma and in accord with principles listed in the Helsinki declaration. Patients were enrolled after informed consent to the employment of biologic samples for research purpose. The surgically resected patient population (Table 1) consisted of 74 males and 26 females, ages between 45 and 84 years. The population of patients treated with nivolumab included 25 males and 1 female (49–85 years old). Tumor stage was scored using the staging system from the 7th American Joint Committee on Cancer (AJCC; ref. 30). Smoking history, histological diagnosis, pathological staging, and mutational status are reported in Table 1. Eight patients from the surgically resected cohort and 3 from nivolumab treated group were excluded from the statistical analysis due to the lack of complete clinical records. Additionally, eight surgically resected patients were excluded due the inadequacy of tissue samples precluding a complete immunohistochemical analysis. Thus, clinicopathologic correlations were allowed in 84 surgically resected and 23 advanced NSCLC cases.

Immunohistochemical analysis

PD-L1. The quantification of PD-L1 expression was assessed after a comparative evaluation between immunoperoxidase and immunofluorescence on control tissues (placenta) and on serial sections from the same case using different anti–PD-L1 antibodies (Extended data in Supplementary Table S1). After careful evaluation and consultation with expert pathologists, reliable and consistent results were obtained using clone 28-8 that was used for further quantitative analysis.

Tissue sections (5 μm thick) were cut from formalin-fixed, paraffin-embedded blocks containing representative tumors and processed for immunohistochemistry (IHC).

Immunoperoxidase: Following the incubation with anti–PD-L1 antibody (clone 28-8), the reaction was revealed by DAB staining and nuclei were counterstained by light hematoxylin. In accordance with a reported approach (31), an algorithm was used to obtain the PD-L1 score (H-score: 0–300), which is computed on the basis of both extent and intensity of PD-L1 staining.

Confocal Immunofluorescence: Sections were double labeled by anti–PD-L1 (clone 28-8) and Pan-Cytokeratin antibody (clone AE1/AE3) followed by FITC- and TRITC-conjugated specific secondary antibody, respectively. Images were digitally captured by confocal microscopy at 200× final magnification using a Zeiss LSM 700 system with Axio Observer. The fractional area occupied by the fluorescent signal and its intensity, expressed as integrated optical density (IOD) per unit area, was then evaluated using a software for image analysis (Image Pro Plus 4.0). Scores were normalized to the exposure time and bit depth at which the images were captured, allowing scores collected at different exposure times to be comparable. Nuclei were counterstained with 4′,6-Diamidine-2′-phenylindole (DAPI).

The antibodies used and magnitude of sampling is reported in Supplementary Tables S1 and S2.

Published OnlineFirst October 26, 2017; DOI: 10.1158/1078-0432.CCR-17-2156

Table 1. Patient population

Resected	SCC ($n = 58$)	ADC ($n = 42$)
Male (M)	51	23
Female (F)	7	19
Age, years (mean ± SD)	70.13 ± 6.52	65.13 ± 7.29
Smoking status		
Nonsmoker	—	9 (2 M, 7 F)
Ex-smoker	34 (32 M, 2 F)	20 (14 M, 6 F)
Smoker	24 (19 M, 5 F)	13 (7 M, 6 F)
Tumor status		
T1	18	11
T2	26	21
T3	14	9
T4	—	1
Nodal status		
N0	28	19
N1	20	9
N2	6	12
Nx	4	2
Stage		
IA	13	7
IB	10	5
IIA	17	9
IIB	9	6
IIIA	9	15
EGFR status[a]		
Mutant	—	7
Wild-type	—	29
KRAS status[b]		
Mutant	—	5
Wild-type	—	22
Nivolumab treated	**SCC ($n = 13$)**	**ADC ($n = 13$)**
Male (M)	13	12
Female (F)	0	1
Age, years (mean ± SD)	69.39 ± 9.73	64.18 ± 9.41
Stage		
IIIB	1	1
IV	12	12
Smoking status		
Nonsmoker	1	1
Ex-smoker	10	5
Smoker	2	7
EGFR status		
Mutant	—	0
Wild-type	—	13
KRAS status		
Mutant	—	4
Wild-type	—	9

[a]6 patients were not tested.
[b]15 patients were not tested.

TILs. Tumor-infiltrating lymphocytes (TIL) were analyzed by the immunohistochemical detection of CD3, CD8, CD4, PD-1, CD25, CD57, and Granzyme B. Immunoperoxidase was performed using an automated staining system (OptiView DAB IHC Detection Kit—Ventana Medical Systems). T lymphocyte subpopulations were also studied by immunofluorescence in order to simultaneously evaluate multiple epitopes. Sections of NSCLC were incubated with primary antibodies followed by specific secondary antibodies. Nuclei were counterstained with DAPI. The list of antibodies used for TILs immunophenotyping is provided in Supplementary Table S1.

TILs were quantified according to specific recommendations (32), and their number and distribution within the neoplastic tissue were assessed following morphometric criteria detailed in Supplementary Materials. Based on their relative incidence, implemented by double immunofluorescence confocal analysis, the ratio of $CD8^{pos}$ cells among the whole population of T ($CD3^{pos}$) lymphocytes (CD8-to-CD3) and the fraction of PD-1 expressing cells over the cytotoxic ($CD8^{pos}$) lymphocytes (PD-1-to-CD8) was computed.

The magnitude of sampling for TILs analysis is reported in Supplementary Table S2.

ALK expression

This analysis involved 27 surgically resected and 11 advanced ADC. In each case, 4-μm-thick sections were obtained from a representative block. Clone D5F3 (Ventana; prediluted) was used to evaluate ALK expression, as previously suggested (33). More details are reported in Supplementary Materials and Methods.

EGFR and *KRAS* mutational analysis

EGFR and *KRAS* mutations were tested in 36 and 27 surgically resected and 13 and 13 advanced ADC cases, respectively. The methodology has been previously described (33) and is detailed in Supplementary Materials and Methods.

Statistical analysis

The χ^2 test was used to test the differences in categorical variables, and the Wilcoxon rank-sum test to detect differences in continuous variables between groups of patients, given that the distribution of data was not normal (Kolmogorov–Smirnov test). The disease-free survival (DFS), overall survival (OS), and progression-free survival (PFS) were estimated by means of the Kaplan–Meier method. DFS was defined as the interval from surgery to the evidence of recurrence disease, or death, or the last date the patient was known to be recurrence-free or alive; OS was defined as the interval from surgery or start of treatment to death from any cause, or the last date the patient was known to be alive; PFS was defined as the interval from start of treatment to the evidence of progressive disease, or death, or the last date the patient was known to be progression-free or alive. Both DFS and OS data were censored at 5 years. Patients treated with nivolumab were categorized in clinical benefit group, including patients with complete (CR) or partial response (PR) or stable disease (SD) lasting at least 6 months according to RECIST criteria version 1.1 (34) and nonresponders (patients with disease progression and stable disease lasting less than 6 months as best response according to RECIST criteria version 1.1, ref. 34).

Log-rank test was performed to determine the difference in survival between groups. DFS and OS data were then analyzed through multivariate models of Cox regression.

Classification and regression tree (CART) analysis identified specific cutoff values that segregated patients by clinical outcomes. *P* value of 0.05 was always considered significant. IBM SPSS Statistics v 24.0 (IBM) and Stata 13 with Cart module (Statacorp) were used to perform the computations for all analyses.

Results

Immune microenvironment in resected patients

Immunohistochemical assessment of PD-L1 expression. This analysis was carried out on sections obtained from 92 resected NSCLC. The variability among and within cases in both membrane and cytoplasmic PD-L1 expression (Fig. 1A and B) required an

Published OnlineFirst October 26, 2017; DOI: 10.1158/1078-0432.CCR-17-2156

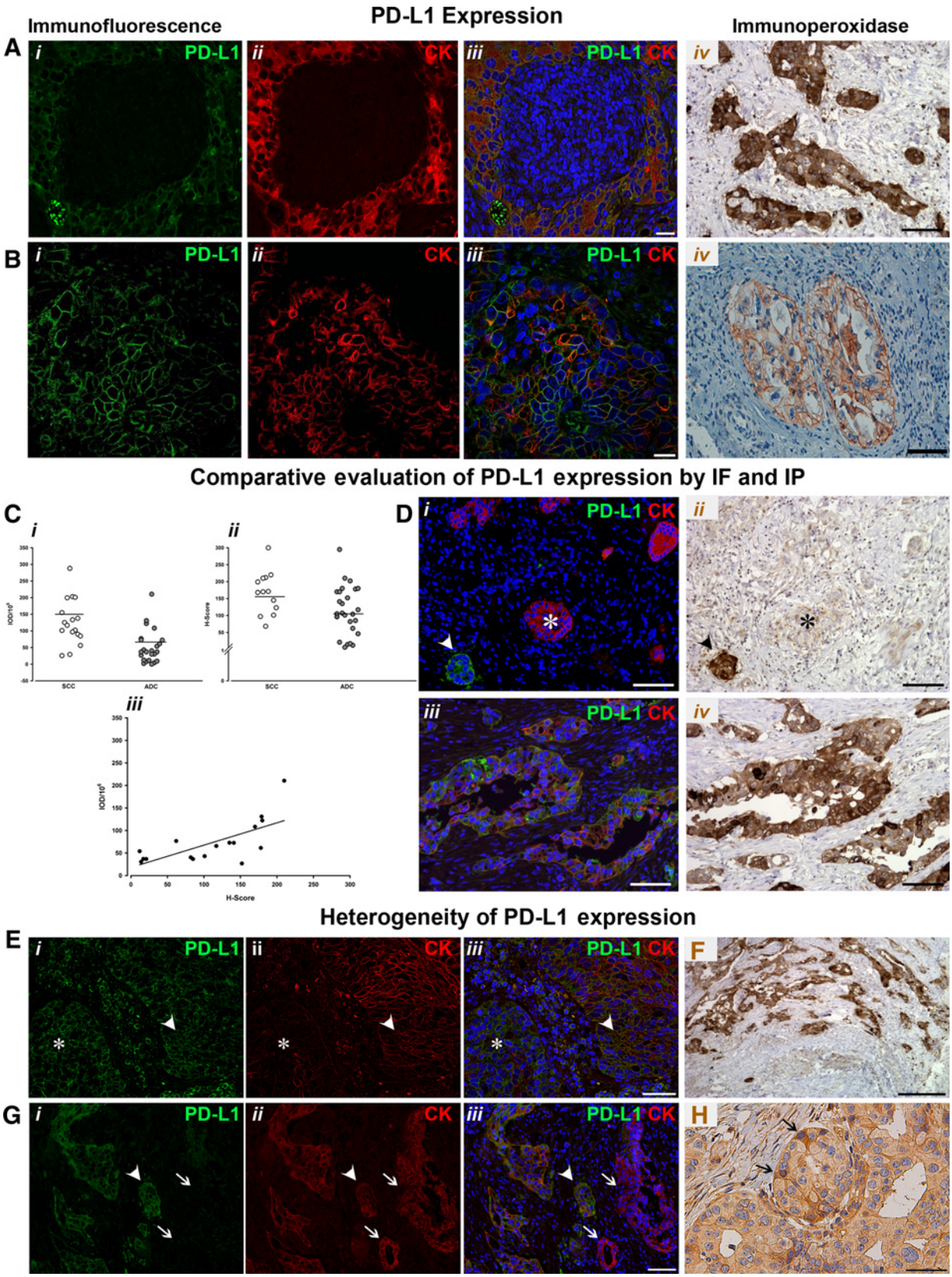

Published OnlineFirst October 26, 2017; DOI: 10.1158/1078-0432.CCR-17-2156

extended sampling to assess the validity of our measurements (Supplementary Table S2).

Based on the extent and intensity of the immune reactivity of PD-L1 in tumors, the H-score was computed on immunoperoxidase-stained sections and expressed as IOD score for quantitative immunofluorescence (QIF; Fig. 1C*i*, C*ii*). A comparative evaluation of PD-L1 expression obtained by IF and IP was performed on serial sections of the same case, documenting that the H-score gradient of intensity measured by IP correlated with IOD values of PD-L1 immunofluorescent signals (Fig. 1C*iii*). Thus, H-score or QIF and their average values were interchangeably used to document the impact of PD-L1 expression on other tested parameters. QIF values were preferentially used when PD-L1 and TILs subpopulations were concurrently considered.

Although a great heterogeneity among and within lung cancer samples (Fig. 1E–G) was observed, average H-score was higher in SCC than in ADC samples (Fig. 1C*ii*) and more than 60% of ADC displayed values below the overall average compared with only 33% of SCC. A significant difference in PD-L1 expression between the two histotypes was confirmed by QIF. SCC specimens exhibited a 2.5-fold higher average PD-L1 value than ADC cases ($P < 0.05$; Fig. 1C*i*).

Specific PD-L1 immunostaining in stromal compartments was also present and involved nearly 10% and 40% of ADC and SCC samples, respectively. However, the significance of PD-L1 in nonneoplastic cells compartments of NSCLC requires a separate study and can only be assessed by an extensive multiple immunofluorescence staining in order to attribute its expression to specific phenotypes.

PD-L1 expression and clinicopathologic features. PD-L1 levels were significantly higher in smokers than in never-smokers and ex-smokers ($P < 0.001$; Supplementary Fig. S1A). In addition, we observed an inverse correlation between PD-L1 expression and N status, as N0 tumors had a 2-fold higher ($P < 0.001$) PD-L1 score compared with N2 (Supplementary Fig. S1B).

At variance with the literature (26, 28), we did not detect a strong association of PD-L1 expression with *EGFR* mutation (n 7/36), while *KRAS* mutated cases (n 5/27) compared with WT displayed lower PD-L1 levels ($P < 0.001$) as measured both by H-score and QIF (Supplementary Fig. S1C).

In our patient population, ALK rearrangement ($n = 27$) was undetectable.

We did not observe statistically significant correlations between PD-L1 expression and other clinical and pathologic features in both NSCLC histotypes.

Thus, tumor PD-L1 values above the average correlated with smoking history and nodal involvement in resected NSCLC patients.

Immunohistochemical analysis of TIL subpopulations. An extensive IHC examination of TILs was carried out in the attempt to assess the contribution of relevant cells in cancer immune landscape, including cytotoxic, helper, and regulatory T cells, and natural killer cells.

The density of lymphocyte subpopulations at tissue level largely reflected the expected incidence according to their phenotype in both NSCLC subsets (Fig. 2A–C); however, a nearly 2-fold increase in $CD3^{pos}$ and a 3-fold reduction in $CD4^{pos}$ TILs were measured in ADC compared with SCC (Fig. 2D, $P < 0.05$). Conversely, no difference was observed in $CD8^{pos}$ lymphocytes density between the two NSCLC histotypes. $CD57^{pos}$ cytotoxic and $CD25/FOXP3^{pos}$ T regulatory cells constituted the lowest subpopulation (Fig. 2E–G) reaching, at most, 2% of TILs. However, compared with ADC, we documented a significant 3-fold increase in $CD57^{pos}$ cells ($P < 0.01$) and a slight increase in $CD25/FOXP3^{pos}$ cells ($P < 0.05$) in SCC cases (Fig. 2H).

According to the different location within the tumor microenvironment, distal $PD\text{-}1^{pos}$ TILs, largely represented at the invasive margin and within germinal centers of tertiary lymphoid structures (TLS; Fig. 2J), appeared to be prominent in SCC cases. Indeed, a significant 1.5-fold increase in the overall number of $PD\text{-}1^{pos}$ lymphocytes was detected in SCC samples compared with ADC (Fig. 2D, $P < 0.05$). In contrast, the quantity of $PD\text{-}1^{pos}$ lymphocytes distributed in intratumor and peritumor (proximal) location, which is expected to be more directly engaged by PD-L1 expressing neoplastic cells, did not significantly vary between the two histotypes (Fig. 2K). Additionally, increasing levels of PD-L1 were coupled by higher frequency of cytotoxic TILs, although this correlation did not reach statistical significance (Supplementary Fig. S2).

Thus, the magnitude and immunophenotype of TILs diverge among NSCLC histotypes, although the fraction of lymphocytes carrying the inhibitory receptor PD-1 located in close contact with neoplastic cells was similar in ADC and SCC samples.

TILs and clinicopathologic features. A statistically significant increase ($P < 0.001$) in $CD8^{pos}$ lymphocytes was measured in T1 compared with T2 NSCLC patients (Supplementary Fig. S3A). In addition, T1 samples showed a consistent reduction in $PD\text{-}1^{pos}$ lymphocytes (Supplementary Fig. S3B $P < 0.001$) with respect to T2 and T3. Accordingly, we documented a significant decrease of

Figure 1.

Images illustrating the diffuse (**A**) and surface (**B**) pattern of PD-L1 expression in sections from surgically resected NSCLC. **A,** The same microscopic field of an ADC case following PD-L1 (green, *i*) and cytokeratin (*ii*, CK, red) immunofluorescent (IF) labeling is merged in *iii* to document by yellowish fluorescence the coexpression of PD-L1 and CK in neoplastic cells. Nuclei are labeled by the blue fluorescence of DAPI. *iv*: The strong diffuse PD-L1 expression (brownish) is also shown by immunoperoxidase (IP). Nuclear counterstaining by light hematoxylin. Similarly, the surface expression of PD-L1 by IF (*i, ii, iii*) and IP (*iv*) is illustrated in **B** in ADC. Scale bars in **A** and **B**: *i, ii, iii* = 50 μm; *iv* = 100 μm. **C,** Dotted plot graphs of the immunohistochemical quantification of PD-L1 expressed as IOD by IF (*i*) or as H-score (0–300) by IP (*ii*). Each dot corresponds to individual IOD and H-score value, whereas lines indicate the average PD-L1 level in SCC (white) and ADC (gray) samples. *iii*: Scatter plot graph illustrating that H-score directly correlates with IOD values (r = 0.57). **D,** PD-L1 labeling by IF (Di, Diii) and IP (Dii, Div) on serial sections from two ADC cases documenting a strong reproducibility among the two methodologies. *i*: *, CK^{pos} (red) neoplastic cells lacking PD-L1 (green) expression, which is confirmed by IP in *ii*. Arrowhead indicates a CK^{neg} neoplastic nodule showing strong PD-L1 (green) expression by both IF and IP. *iii* and *iv*: A comparable PD-L1 labeling by IF and IP is documented on serial sections also showing that only a fraction of neoplastic cells are CK^{pos} and $PD\text{-}L1^{pos}$ (yellow fluorescence). Scale bars, 100 μm. **E** and **G,** Confocal IF images of the same microscopic field of SCC (**E**) and ADC (**G**) samples following PD-L1 (*i*, green) and CK (*ii*, red) IF labeling are merged in *iii*, respectively. Arrowheads indicate CK^{pos} and $PD\text{-}L1^{pos}$ tumor cells; *, a neoplastic area with strong PD-L1 expression and weak or negative CK signal. Arrows point to CK^{pos} tumor cells that are negative for PD-L1. The variability of PD-L1 expression was also documented by IP in different areas of the same case (**F**) as within the same neoplastic nodule (**H**), in which arrows point to neoplastic cells strongly positive for PD-L1. Scale bars, **E** and **H** = 50 μm; **F** = 250 μm; **G**: 100 μm.

Published OnlineFirst October 26, 2017; DOI: 10.1158/1078-0432.CCR-17-2156

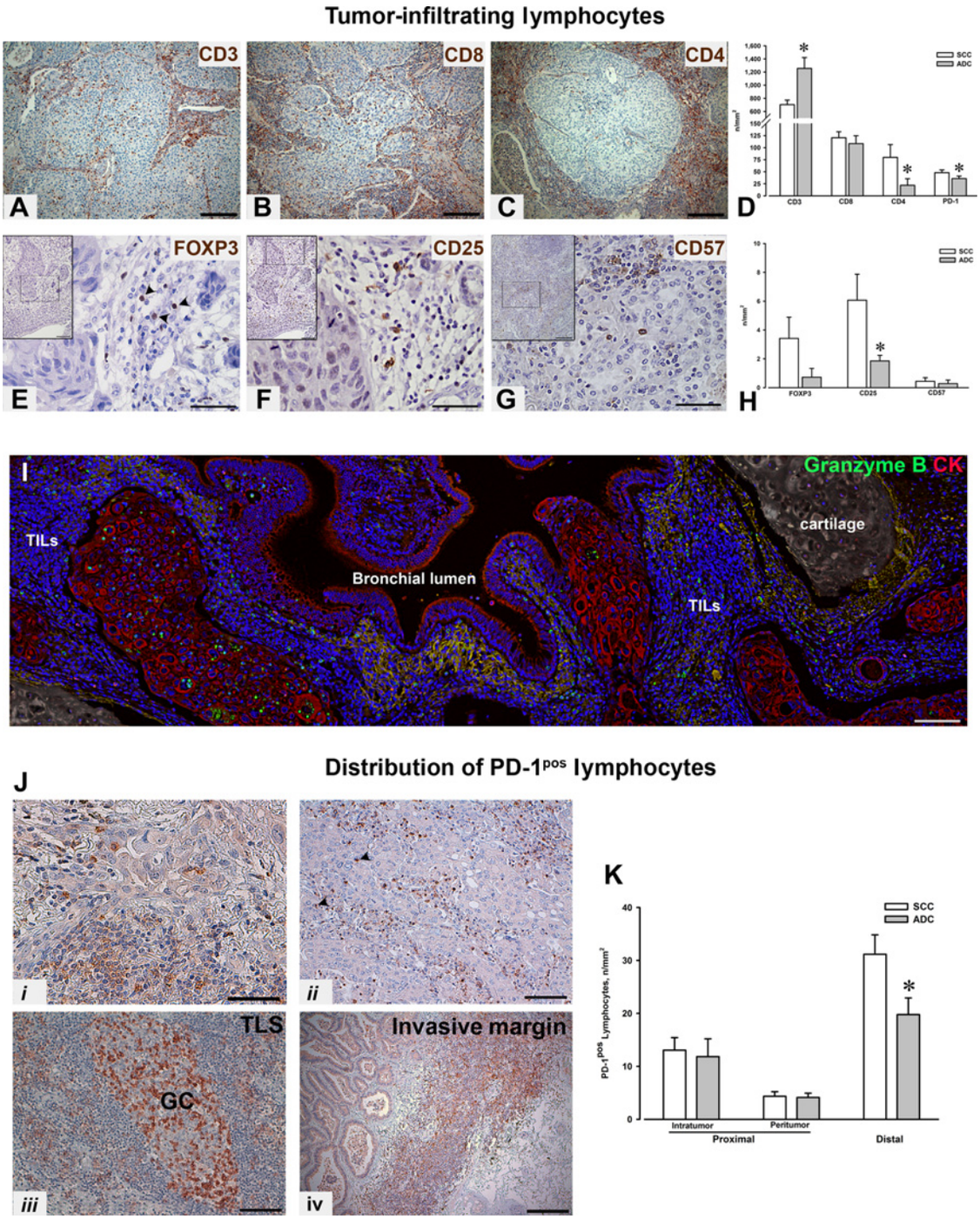

Figure 2.

Immunohistochemical detection of TIL subpopulations in NSCLC. Immunoperoxidase staining (brownish) of CD3 (**A**), CD8 (**B**), and CD4 (**C**) documenting TILs surrounding neoplastic nodules. Scale bars, **A–C** = 200 μm. **D,** Bar graph of the quantification of TILs in SCC (white) and ADC (gray) cases according to lymphocyte subsets. *, $P < 0.05$ vs. SCC. **E** and **F,** Serial sections from an SCC case to show, in the same microscopic field, FOXP3 (**E**) and CD25 (**F**) immunostaining. At low magnification (insets), the two areas inscribed by white rectangles are illustrated at higher magnification to highlight the nuclear labeling of FOXP3 (arrowheads) and membrane expression of CD25 in T regulatory cells. **G,** Differentiated NK cells labeled by CD57 infiltrating the neoplastic tissue are illustrated at low (inset) and high magnification. Scale bars, **E–G**, insets, 100 μm; main images, 50 μm. **H,** Bar graph of the quantification of FOXP3, CD25, and CD57 immunolabeling in SCC (white) and ADC (gray). *, $P < 0.05$ vs. SCC. **I,** This image corresponds to a section from an ADC case in which the cytotoxic molecule Granzyme B (green) is abundantly expressed by TILs in neoplastic areas recognized by the red fluorescence of CK. Lower expression of Granzyme B is apparent in a neoplastic structure bulging the bronchial lumen (*). Scale bar, 100 μm. **J,** Sections from SCC case documenting the different distribution of PD-1^{pos} TILs within the tumor microenvironment. *i, ii*: Proximal lymphocytes were considered when in intratumor (arrowheads) or peritumor localization. Distal PD-1^{pos} lymphocytes (*iii*) were predominantly located in germinal center (GC) of TLS and in proximity of the tumor invasive margin (*iv*). Scale bars: *i, ii* = 50 μm; *iii* = 100 μm; and *iv* = 200 μm. **K,** Bar graph of the quantification of PD-1^{pos} lymphocytes according to their localization in samples from the two histotypes. *, $P < 0.05$ vs. SCC.

PD-1^{pos} lymphocytes in N0 cases compared with N1 ($P < 0.001$) and N2 ($P < 0.001$; Supplementary Fig. S3C). As a result of these findings, PD-1^{pos} lymphocytes were 2-fold lower in stage I NSCLC compared with stage II ($P < 0.001$) and III ($P < 0.001$; Supplementary Fig. S3D), and ADC samples displayed an increasing PD-1 gradient ($P < 0.001$) according to the severity of the disease (Supplementary Fig. S3E). When the smoking history was considered, in SCC cases, smokers showed higher average values ($P < 0.01$) of PD-1^{pos} lymphocytes (mean ± SE: 53.7 ± 8.8) compared with ex-smokers (mean ± SE: 38.1 ± 11.35).

No significant association of TILs values with demographic parameters was observed. However, *EGFR* and *KRAS* mutations appeared to condition a significant reduction of CD8^{pos} and PD-1^{pos} cells and a different tissue localization of PD-1^{pos} lymphocytes resulting in lower intratumor density compared with WT cases ($P < 0.05$; Supplementary Fig. S3F). No differences were observed in the amount of PD-1^{pos} cells located at the invasive margin according to the mutational status.

Thus, a strong association of TILs number and PD-1 distribution with clinicopathologic characteristics was documented in our cohort of resected NSCLC, supporting their clinical relevance.

The landscape of NSCLC immune microenvironment. We reasoned that a comprehensive definition of NSCLC immune microenvironment would have enhanced the biologic and clinical significance of our findings.

Thus, a more complex analysis of the tumor microenvironment was conducted considering the PD-L1 status together with the magnitude and phenotype of TILs involvement. Based on a well-described literature (29) and a recently proposed classification (28), we divided our cases into four categories: type I adaptive immune resistance, type II immune ignorance, type III intrinsic induction, and type IV immune tolerance. By this approach, we documented that more than one third of NSCLC samples displayed a type II contexture, likely reflecting immune exhaustion at the time of diagnosis, while a similar proportion of type III and IV was observed (Supplementary Fig. S4A and S4B). The impact on clinical outcome of this more coordinate contribution of both tumor and TILs was apparent. NSCLC with high PD-L1 score and low TILs (type III) had the longest OS (75th percentile of survival time = 37 ± 16.22 months) and DFS (75th percentile of survival time = 11 ± 3.45 months) while type II immune ignorant cases were associated with worst prognosis (OS: 75th percentile of survival time = 16 ± 6.21 months; DFS: 75th percentile of survival time = 8 ± 2.03 months).

Thus, the overall estimation of PD-L1 in cancer cells and TILs allows the identification of immune tissue characteristics with impact on clinical parameters. However, the low statistical power documented by the Kaplan–Meier curve (Supplementary Fig. S4C), of such an unrefined classification of NSCLC environments prompted us to test whether individual or, more likely, a combination of multiple tissue parameters would have significant prognostic and predictive value in surgically resected patients.

Tissue immunophenotypic signatures with clinical impact

PD-L1 expression did not show a statistical significant impact on survival at univariate analysis (Table 2), although the percentage of survivors was higher (OS: 77%; DFS: 27%) in NSCLC patients with PD-L1 values above the average compared with PD-L1 low group (OS: 58%; DFS: 18%; Supplementary Table S4).

On univariate analysis also, TIL density did not show a statistical significant impact on survival (Table 2). However, higher percentage of survivors were documented in ADC samples rich in CD3^{pos} (OS: 65%; DFS: 37%) and in CD8^{pos} (OS: 65%; DFS: 21%) lymphocytes with respect to CD3, poor (OS: 45%; DFS: 3%) and CD8, poor (OS: 43%; DFS: 9%) cases (Supplementary Table S4).

Similarly, in the overall population of NSCLC patients low tissue density of PD-1^{pos} lymphocytes was associated to a higher fraction of disease free survivors (DFS: 22%) compared with the PD-1 high counterpart (DFS: 0%; Supplementary Table S4).

Conversely, more defined immunophenotypic features appeared to strongly predict the clinical outcome on both univariate and multivariate analysis. Specifically, the proportion of CD8^{pos} cells among the overall population of CD3^{pos} TILs and the fraction of cytotoxic lymphocytes lacking the inhibitory receptor PD-1 were candidate to better represent the population of antitumor effector lymphocytes.

As shown in Table 2, high CD8-to-CD3 ratio was positively correlated with OS and DFS (OS: HR = 0.965, 95% CI, 0.931–1.001, $P = 0.057$; DSF: HR = 0.954, 95% CI, 0.965–0.983, $P = 0.002$) on univariate analysis, although not reaching statistical significance on multivariate analysis. The Kaplan–Meier curve documented longer OS in patients with high CD8-to-CD3 ratio (Fig. 3C; HR: 0.542, 95% CI, 0.260–1.133, $P = 0.096$).

The impact of PD-1-to-CD8 ratio on clinical outcome was striking. This parameter resulted an independent predictor of OS in both univariate (OS: HR = 1.952, 95% CI, 1.34–3.12, $P = 0.001$) and multivariate analysis (OS: HR = 1.943, 95% CI, 1.38–2.86, $P = 0.009$) while its impact on DFS was seen only on univariate test (DSF: HR = 1.537, 95% CI, 1.12–2.10, $P = 0.007$). Importantly, the Kaplan–Meier curve showed longer OS (HR: 2.268, 95% CI, 1.056–4.871, $P = 0.03$) in patients with low PD-1-to-CD8 ratio (Fig. 3D).

Clinicopathologic features such as age and histotype also had, to some extent, statistical significant impact on survival (Table 2). On univariate analysis, only the N status significantly correlated with OS and DFS (OS: HR = 1.87, 95% CI, 1.2–2.91, $P = 0.004$; DFS: HR = 1.524, 95% CI, 1.057–2.195, $P = 0.02$) while on multivariate model statistical significance was maintained only on OS (OS: HR = 1.86, 95% CI, 1.31–3.96, $P = 0.015$; Table 2). Based on this finding, patients were clustered according to the combination of the two most powerful statistical parameters detected in our patient population of NSCLC. As shown by the Kaplan–Meier curve (Fig. 3F), cases carrying N 0 tumors and low tissue PD-1-to-CD8 ratio had a statistically significant longer OS (HR: 1.624, 95% CI, 1.148–2.296, $P = 0.006$) compared with other parametric combinations. Importantly, worst prognosis was seen in patients whose samples displayed high number of CD8^{pos} lymphocytes expressing PD-1, independently from the N status. Thus, the tissue content of cytotoxic TILs carrying the inhibitory receptor PD-1 appeared to limit the prognostic value of N status (Fig. 3F).

Immune microenvironment in patients treated with nivolumab

In the attempt to define not only the prognostic role, but also the potential predictive value of the immune microenvironment on the response to ICI, a similar analysis was performed on a selected group of 26 NSCLC patients receiving anti PD-1

Published OnlineFirst October 26, 2017; DOI: 10.1158/1078-0432.CCR-17-2156

Table 2. Explanatory prognostic factors in a Cox proportional hazards model

	Univariate[a]			Multivariate[b]		
	HR (95% CI)	χ^2	***P***	**HR (95% CI)**	χ^2	***P***
Overall survival						
Sex	1.969 (0.973–3.987)	3.677	0.06	1.099 (0.437–2.764)		0.842
Age	0.977 (0.319–0.977)	0.990	0.319	1.043 (0.976–1.114)		0.213
Smoking	0.983 (0.578–1.670)	0.004	0.949			
Histotype	0.564 (0.286–1.113)	2.803	0.097	0.807 (0.332–2.360)		0.885
Grading	1.127 (0.525–2.417)	0.094	0.759			
Staging	1.228 (0.986–1.530)	3.399	0.065			
N status	1.87 (1.201–2.911)	8.095	**0.004**	1.863 (1.131–3.068)		**0.015**
PD-L1						
QIF	1.00 (1.00–1.00)	0.389	0.534			
H-score	0.99 (0.991–1.007)	0.06	0.807			
CD3	1.00 (1.00–1.00)	0.064	0.80			
CD8	0.999 (0.995–1.003)	0.192	0.661			
CD8/CD3	0.965 (0.931–1.001)	4.432	0.057	0.979 (0.942–1.017)		0.282
PD-1	1.01 (0.989–1.014)	0.042	0.838			
PD-1/CD3	0.860 (0.20–6.795)	0.006	0.937			
PD-1/CD8	1.952 (1.335–2.852)	13.642	**0.001**	1.804 (1.155–2.816)		**0.009**
Disease-free survival						
Sex	1.82 (1.01–3.288)	4.094	**0.046**	0.689 (0.314–1.511)		0.352
Age	0.935 (0.894–0.978)	8.542	**0.03**	0.998 (0.941–1.058)		0.948
Smoking	0.852 (0.555–1.306)	0.541	0.462			
Histotype	0.287 (0.159–0.518)	19.235	**<0.001**	0.584 (0.272–1.254)		0.168
Grading	0.788 (0.448–1.386)	0.689	0.408			
Staging	1.177 (0.973–1.424)	2.827	0.094			
N status	1.524 (1.057–2.195)	5.229	**0.024**	1.464 (0.990–2.165)		0.056
PD-L1						
QIF	1.00 (1.00–1.00)	2.849	0.094			
H-score	0.996 (0.990–1.002)	1.923	0.166			
CD3	1.00 (1.00–1,00)	0.880	0.350			
CD8	0.997 (0.993–1.001)	2.534	0.112			
CD8/CD3	0.954 (0.925–0.983)	9.471	**0.002**	0.966 (0.932–1.001)		0.055
PD-1	0.999 (0.989–1.008)	0.055	0.815			
PD-1/CD3	0.122 (0.003–4.741)	0.878	0.260			
PD-1/CD8	1.537 (1.124–2.102)	7.717	**0.007**	1.236 (0.890–1.716)		0.207

NOTE: Sex (male = 0, female = 1), smoking status (0 = history negative for smoking, 1 = history positive for smoking), and histotype (SCC = 0, ADC = 1). Continue variables: age, grading, staging, N status, PD-L1 expression, CD3, CD8, CD8-to-CD3, PD-1, PD-1-to-CD3, and PD-1-to-CD8. Statistical results with $P < 0.05$ are bolded.

[a]Univariate analysis is carried out without any adjustment.

[b]In addition to clinically relevant variables, multivariate analysis is carried out on statistically significant parameters obtained from the univariate model.

(nivolumab) treatment (Fig. 4A–C). Nine patients (35%) were included in the clinical benefit group (CR and PR, an SD lasting 6 months at least) according to RECIST criteria (34), while the remaining 17 patients had progression of disease at first tumor assessment.

PD-L1 expression was high in 55% of patients within the clinical benefit group versus 42.5% in nonresponders ($P = 0.225$).

In strong agreement with our previous findings, 100% of nivolumab treated patients with clinical benefit displayed low PD-1-to-CD8 ratio compared with 21.4% of nonresponders ($P < 0.001$; Fig. 4D). High CD8-to-CD3 ratio was present in 55.6% of patients within the clinical benefit group and in 42.8% of nonresponders ($P = 0.098$). In addition, 66.6% of cases belonging to the clinical benefit group showed low number of PD-1^{pos} lymphocytes compared with 64.2% of nonresponders ($P = 0.74$). Importantly, although not reaching a statistically significant impact on OS (Fig. 4G and H), we documented a longer PFS (HR = 2.728, 95% CI, 0.967–7.697, $P = 0.047$) in cases with high CD8-to-CD3 ratio (median PFS = 4.24 months) versus low (median PFS = 1.81 months) and a significant prolonged PFS (HR = 4.51, 95% CI, 1.459–13.944, $P = 0.004$) in patients with low (median PFS = 12.96 months) versus high (median PFS = 1.84 months) PD-1-to-CD8 ratio (Fig. 4E and F).

Our data suggest that the amount of residual PD-1–negative cytotoxic effectors TILs may be considered a potential predictive factor in NSCLC patients treated with nivolumab.

Discussion

Blockade of inhibitory immune checkpoints is currently arising as a promising option of anticancer strategies. Targeting the PD-1/PD-L1 pathway has shown encouraging results on various malignancies (9, 35–37) and has changed the standard of care in first- and second-line therapy of advanced NSCLC (5, 6, 10–12). In this clinical setting, reliable predictive biomarkers are the object of significant financial investments although are difficult to obtain due to the complex tumor–host relationship. The actual assessment of risk stratification according to clinicopathologic (38) and biomolecular (39) parameters although showing relevant prognostic impact in NSCLC could be integrated with immunologically defined factors. It is also increasingly clear that the development of biomarkers for anti–PD-1/PD-L1 therapy requires a better understanding of PD-L1 expression profile and its interaction with TILs. It cannot be underestimated that these biomarker-oriented efforts will provide important insights into the pathogenesis and progression of NSCLC.

Published OnlineFirst October 26, 2017; DOI: 10.1158/1078-0432.CCR-17-2156

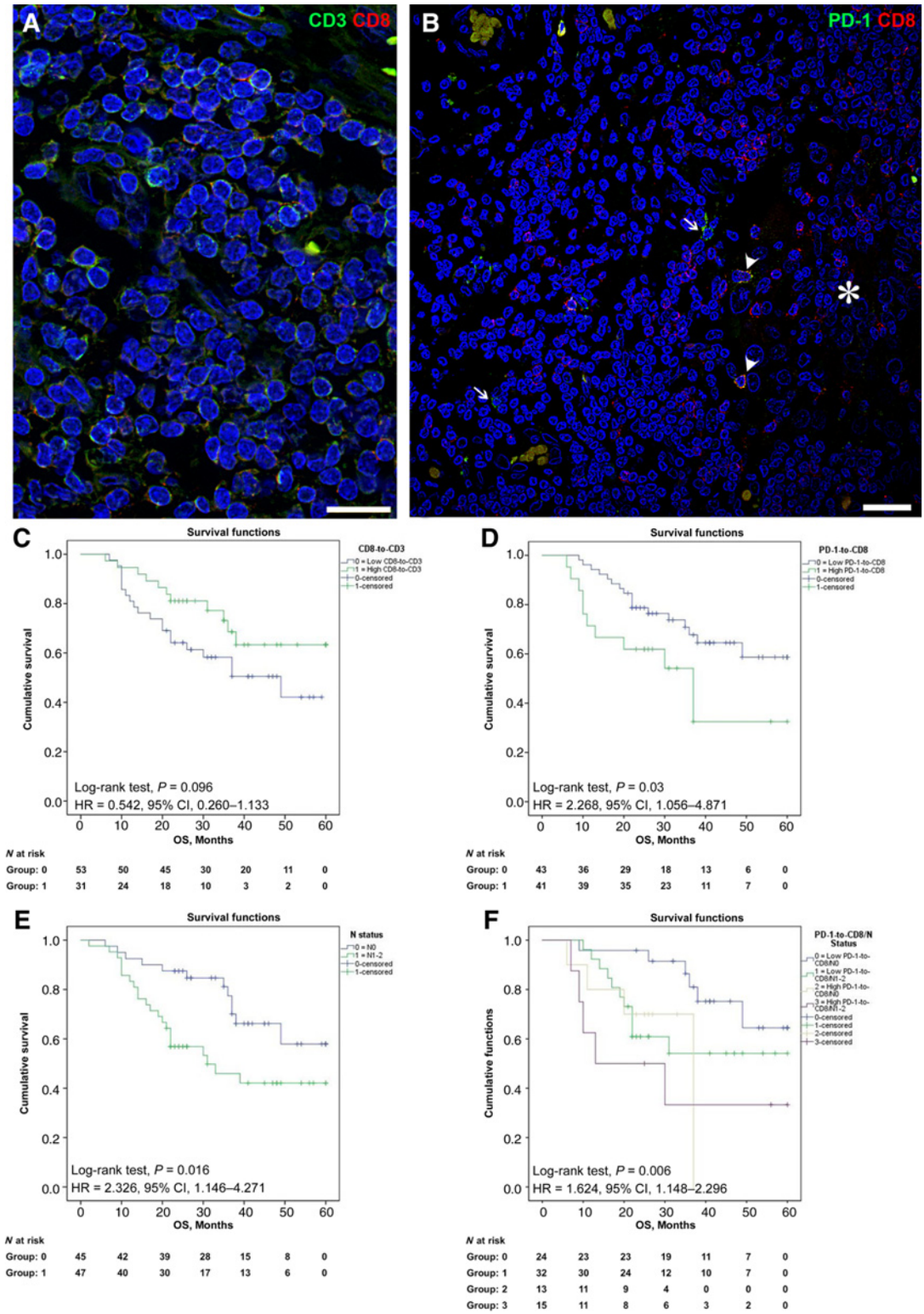

Figure 3.

A, Double immunofluorescence staining for CD3 (green) and CD8 (red) in a section from NSCLC. Yellowish fluorescence corresponds to the co-expression of the two antigens. **B,** Confocal images of double immunolabeling for the detection of PD-1 (green) and $CD8^{pos}$ (red) lymphocytes in a cluster of TILs surrounding and infiltrating "bona fide" neoplastic cells (*). Arrowheads point to $PD\text{-}1^{pos}$ $CD8^{pos}$ TILs documented by bright fluorescence, whereas arrows indicate lymphocytes labeled by PD-1 only. Scale bars: **A**, 20 μm; **B**, 30 μm. **C–F,** Kaplan–Meier survival curves illustrating the prognostic effect on OS of CD8-to-CD3 (**C**), PD-1-to-CD8 (**D**), nodal involvement (**E**), and its combination with PD-1-to-CD8 (**F**) in surgically resected NSCLC cases. Number at risk is reported at the bottom of each curve.

Published OnlineFirst October 26, 2017; DOI: 10.1158/1078-0432.CCR-17-2156

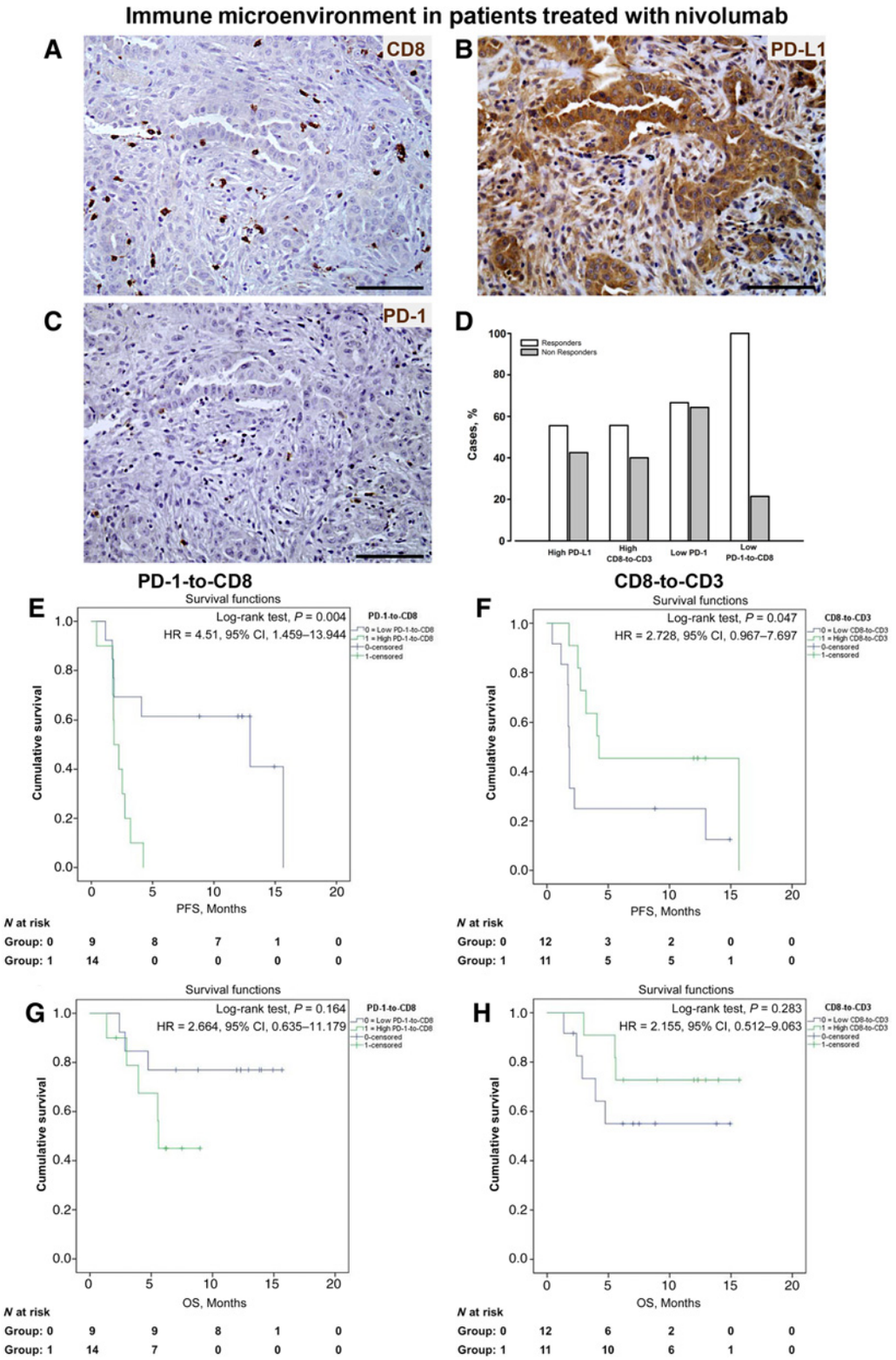

Figure 4.

Serial sections from an ADC patient treated with nivolumab belonging to the clinical benefit group, documenting in the same microscopic field CD8 (**A**) and PD-1 (**C**) labeled lymphocytes infiltrating neoplastic structures showing strong PD-L1 expression (**B**). PD-L1 staining is also present within the stromal tissue. Scale bars, 100 μm. **D,** Bar graph documenting the percent distribution of NSCLC patients treated with nivolumab, among the clinical benefit group (white) and nonresponders (gray), according to different parameters of the immune microenvironment. **E–H,** Kaplan–Meier curves showing the predictive effect of PD-1-to-CD8 (**D**, **F**) and CD8-to-CD3 (**E**, **G**) on DFS (**D**, **E**) and OS (**F**, **G**), respectively, in advanced NSCLC treated with immunotherapy. Number at risk is reported at the bottom of each curve.

Published OnlineFirst October 26, 2017; DOI: 10.1158/1078-0432.CCR-17-2156

In order to prospectively evaluate the prognostic impact of different subpopulations of TILs and PD-L1 expression, we performed a retrospective systematic tissue analysis on a well-defined cohort of 100 stage I to IIIa NSCLC patients undergoing primary tumor resection without previous neoadjuvant therapy and 26 advanced NSCLC patients treated with nivolumab.

Although the original aim of our study was not to deliver a novel translatable biomarker, the simultaneous assessment of the prominent actors of NSCLC immune editing, surveillance, and escape allowed us to identify immune tissue contexts with differential impact on clinical outcome. Specifically, we documented that the reservoir of an efficient population of cytotoxic cells lacking PD-1 receptor is a potential independent prognostic and predictive variable in NSCLC. Thus, low PD-1-to-CD8 ratio resulted in longer OS and DFS in resected patients as was able to predict tumor response to nivolumab. These findings are in agreement with the expected positive clinical impact of a locally active TIL population tackling on cancer growth and progression. Interestingly, our data are in accordance with the recent identification in human and experimental NSCLC (40), and in melanoma patients (41) of a tissue and circulating subpopulation of exhausted lymphocytes that can be rescued by anti–PD-1-targeted drugs. These $CD8^{pos}$ cells expressing the costimulatory molecule CD28 undergo active replication ($Ki67^{pos}$) following anti–PD-1 blockade. Intriguingly, the immunophenotype of these cells also involves PD-1, pointing to the dual activating and inhibitory function of the receptor (40). Importantly, the presence of a similar lymphocyte subpopulation within the neoplastic tissue was documented in NSCLC and melanoma patients by immunophenotyping (41) and clonal analysis of T-cell receptor (TCR) repertoire (42), respectively. Our immunohistochemical approach makes it difficult to dissect whether PD-1 carrying lymphocytes predominantly undergo anergy or shift toward an activating pathway. However, based on our multiparametric clinicopathologic correlation, it is likely that PD-1 expressing TILs were mostly directed to a PD-L1–mediated inhibitory fate. Overall, these findings underline the need to define which subpopulation of TILs expresses PD-1 and whether and to which extent PD-1 expression reflects activation or inhibition. Finally, we are encouraged to support PD-1-to-CD8 ratio as a potential biomarker by the first approved clinical trial applying the CRISPRcas technology in lung cancer, in which PD-1 inhibitory receptor has been genetically disrupted in adoptive cell transfer (43).

In addition, specific subpopulations of TILs strongly correlated with clinicopathologic parameters. Thus, T1 tumors had high CD8 and low PD-1 content and N0 cases were characterized by low number of tissue $PD\text{-}1^{pos}$ cells. Taken together, an inverse correlation between the number of $PD\text{-}\ 1^{pos}$ TILs and NSCLC clinical staging was observed (Supplementary Fig. S3). In our cohort of patients, the mutational status, including *EGFR* and *KRAS* mutation, had an impact on TILs. Specifically, *EGFR* mutation appeared to condition a significant reduction in $CD8^{pos}$ and $PD\text{-}1^{pos}$ cells and a different tissue distribution of $PD\text{-}1^{pos}$ lymphocytes resulting in lower intratumor density compared with WT cases. In agreement with the literature (44), we documented a reduction in the numerical incidence of TILs carrying PD-1 receptor in patients with *KRAS* mutation compared with WT. The lack of *ALK* rearrangement in our patient population does not allow to discuss potential correlations with the immunophenotypic changes of TILs.

Our data are in line with the general view that high PD-L1 expression conditions a better outcome in NSCLC (18). In this regard, although PD-L1 did not possess a strong statistical power as an individual prognostic factor on univariate analysis, higher levels of expression were associated with prolonged OS and DFS. Moreover, a significant correlation between high PD-L1 tumor content and low N status was documented in our cohort of patients.

A great inter- and intrapatient variability of PD-L1 levels was confirmed by our immunohistochemical analysis, suggesting the involvement of several factors in shaping the expression of this protein. Inflammatory (45) and genetic (23, 24) backgrounds are known to condition tumor PD-L1 expression. In this regard, in our NSCLC samples, higher levels of PD-L1 were detected in the presence of an active cytotoxic TILs population as documented by a predominant CD8 phenotype (Supplementary Fig. S2). These cells are likely responsible for IFNγ secretion, the most powerful PD-L1 stimulating factor (45). Secondly, *KRAS* mutation was associated with a reduced expression of PD-L1, as previously documented (44), while, at variance with the literature (26, 46), *EGFR* mutation did not statistically impact on this parameter. It has been extensively reported that tumors with a greater mutational load could generate more neoantigens leading to a larger repertoire of tumor-specific T cells (41). However, epigenetic mechanisms leading to elevated expression of non-mutated self-antigens could confer high tumor antigenicity despite a low number of mutations (4). Accordingly, recent experimental observations and ongoing clinical trials have been addressed to determine whether the combination of two ICI or the association of ICI with chemotherapy or vaccination (47, 48) are able to induce a specific reinvigoration of T $CD8^{pos}$ lymphocytes. Finally, we observed morphologically recognizable neoplastic areas showing low or absent epithelial markers in the presence of high level of PD-L1 expression (Fig. 1E and G). These findings suggest additional roles of PD-L1 in tumor biology, including epithelial to mesenchymal transition (EMT; ref. 49).

The present investigation highlights the notion that ADC and SCC have a different biologic and tissue background (28, 50), including the immune context. In this regard, we documented that 36% of SCC samples displayed type III intrinsic induction, while in ADC the proportion of type IV and II was consistently higher (32% and 36%, respectively). Additionally, ADC displayed a lower expression of PD-L1 while, in line with other observations (26), the microenvironment seemed to be more chemoattractive for the overall population of T lymphocytes than in SCC. Accordingly, the clinical outcome of our cohort of surgically resected patients consistently varied between the two histotypes in terms of DFS that was considerably higher in SCC compared with ADC (28 months vs. 13 months, $P < 0.001$).

Some limitations of our study have to be acknowledged. First, the early stage of the disease of our patient population may restrain the wide application of our findings to the prevalent cohort of unresectable and more advanced NSCLC. Although the overall number of cases studied is relatively limited, potentially attenuating our conclusive remarks, patients had an adequate follow up (60 months) since only 10% were collected in 2015. We have to point out that the lack of functional test and an incomplete analysis of other relevant immune cells, as tumor associated macrophages and dendritic cells, may reduce the claim of fully defined immune contexts.

Published OnlineFirst October 26, 2017; DOI: 10.1158/1078-0432.CCR-17-2156

Thus, our efforts are presently addressed to extend the functional characterization of the tumor microenvironment and the role of myeloid derived suppressors cells (MDSC) whose analysis, conversely, represents a challenge due to their complex phenotype. Additionally, to strengthen the predictive value of our proposed biomarker, further analysis in a larger population of patients treated with ICI is required.

As a final consideration, we believe that an accurate pathological evaluation is still a fundamental tool to interpret molecular, cellular and tissue analysis of the immune reaction against tumor. Therefore, an extended and integrated approach as described here to define multiple variables contributing to cancer microenvironment is necessary in the current stage of our understanding of PD-1/PD-L1 immune checkpoint and its therapeutic targeting.

In the context of PD-L1 activation, a high fraction of cytotoxic CD8 lymphocytes lacking the inhibitory receptor PD-1 is a potential positive prognostic and predictive factor in NSCLC. Importantly, this population of effector cells can be fostered by PD-1 targeting drugs. Our study also raises the question whether the current indications for ICI treatment may be expanded, opening the possibility to include earlier stages of the disease. Indeed, neoadjuvant and adjuvant ICI trials are undergoing with the expectation that precocious interventions may restore an active surveillance against cancer, preventing the natural switch of NSCLC immune microenvironment to a silent unfavorable fate.

Disclosure of Potential Conflicts of Interest

No potential conflicts of interest were disclosed.

Authors' Contributions

Conception and design: G. Mazzaschi, G. Bocchialini, F. Aversa, F. Quaini, M. Tiseo

Development of methodology: D. Madeddu, A. Falco, C.A. Lagrasta, K. Urbanek

Acquisition of data (provided animals, acquired and managed patients, provided facilities, etc.): G. Mazzaschi, D. Madeddu, A. Falco, G. Bocchialini, F. Sogni, G. Armani, C.A. Lagrasta, B. Lorusso, C. Mangiaracina, R. Vilella, C. Frati, L. Ampollini, M. Veneziani, K. Urbanek, F. Quaini, M. Tiseo

Analysis and interpretation of data (e.g., statistical analysis, biostatistics, computational analysis): G. Mazzaschi, M. Goldoni, C.A. Lagrasta, L. Ampollini, F. Quaini, M. Tiseo

Writing, review, and/or revision of the manuscript: G. Mazzaschi, D. Madeddu, R. Alfieri, F. Aversa, F. Quaini, M. Tiseo

Administrative, technical, or material support (i.e., reporting or organizing data, constructing databases): G. Mazzaschi, D. Madeddu, C.A. Lagrasta, E.M. Silini

Study supervision: G. Mazzaschi, C.A. Lagrasta, E.M. Silini, A. Ardizzoni, F. Aversa, F. Quaini

Acknowledgments

The authors gratefully thank Emilia Corradini, Gabriella Becchi, and Nicoletta Campanini for their invaluable technical assistance. This work was supported by Associazione Italiana per la Ricerca sul Cancro (AIRC) grants IG 14214 to M. Tiseo and IG 2016 Id 19026 to A. Ardizzoni.

The costs of publication of this article were defrayed in part by the payment of page charges. This article must therefore be hereby marked *advertisement* in accordance with 18 U.S.C. Section 1734 solely to indicate this fact.

Received July 27, 2017; revised September 13, 2017; accepted October 23, 2017; published OnlineFirst October 26, 2017.

References

1. Hanahan D, Weinberg RA. Hallmarks of cancer: the next generation. Cell 2011;144:646–74.
2. Vesely MD, Kershaw MH, Schreiber RD, Smyth MJ. Natural innate and adaptive immunity to cancer. Annu Rev Immunol 2011;29:235–71.
3. Pardoll DM. The blockade of immune checkpoints in cancer immunotherapy. Nat Rev Cancer 2012;12:252–64.
4. Rizvi NA, Hellmann MD, Snyder A, Kvistborg P, Makarov V, Havel JJ, et al. Mutational landscape determines sensitivity to PD-1 blockade in non–small cell lung cancer. Science 2015;348:124–8.
5. Brahmer J, Reckamp KL, Baas P, Crinò L, Eberhardt WE, Poddubskaya E, et al. Nivolumab versus docetaxel in advanced squamous-cell non-small-cell lung cancer. N Engl J Med 2015;373:123–35.
6. Borghaei H, Paz-Ares L, Horn L, Spigel DR, Steins M, Ready NE, et al. Nivolumab versus docetaxel in advanced nonsquamous non-small-cell lung cancer. N Engl J Med 2015;373:1627–39.
7. Kwak EL, Bang YJ, Camidge DR, Shaw AT, Solomon B, Maki RG, et al. Anaplastic lymphoma kinase inhibition in non-small-cell lung cancer. N Engl J Med 2010;363:1693–703.
8. Mok TS, Wu YL, Thongprasert S, Yang CH, Chu DT, Saijo N, et al. Gefitinib or carboplatin-paclitaxel in pulmonary adenocarcinoma. N Engl J Med 2009;361:947–57.
9. Herbst RS, Baas P, Kim DW, Felip E, Pérez-Gracia JL, Han JY, et al. Pembrolizumab versus docetaxel for previously treated, PD-L1-positive, advanced non-small-cell lung cancer (KEYNOTE-010): a randomised controlled trial. Lancet 2016;387:1540–50.
10. Rittmeyer A, Barlesi F, Waterkamp D, Park K, Ciardiello F, von Pawel J, et al. Atezolizumab versus docetaxel in patients with previously treated non-small-cell lung cancer (OAK): a phase 3, open-label, multicentre randomised controlled trial. Lancet 2017;389:255–65.
11. Herbst RS, Soria JC, Kowanetz M, Fine GD, Hamid O, Gordon MS, et al. Predictive correlates of response to the anti-PD-L1 antibody MPDL3280 in cancer patients. Nature 2014;515:563–7.
12. Aguiar PN Jr, De Mello RA, Hall P, Tadokoro H, Lima Lopes G. PD-L1 expression as a predictive biomarker in advanced non-small-cell lung cancer: updated survival data. Immunotherapy 2017;9:499–506.
13. Gibney GT, Weiner LM, Atkins MB. Predictive biomarkers for checkpoint inhibitor-based immunotherapy. Lancet Oncol 2016;17:e542–51.
14. Kluger HM, Zito CR, Turcu G, Baine MK, Zhang H, Adeniran A, et al. PD-L1 studies across tumor types, its differential expression and predictive value in patients treated with immune checkpoint inhibitors. Clin Cancer Res 2017. doi: 10.1158/1078-0432.CCR-16-3146.
15. Zhou C, Tang J, Sun H, Zheng X, Li Z, Sun T, et al. PD-L1 expression as poor prognostic factor in patients with non-squamous non-small cell lung cancer. Oncotarget 2017. doi: 10.18632/oncotarget.17022.
16. Sorensen SF, Zhou W, Dolled-Filhart M, Baehr Georgsen J, Wang Z, Emancipator K, et al. PD-L1 expression and survival among patients with advanced non–small cell lung cancer treated with chemotherapy. Transl Oncol 2016;9:64–9.
17. McLaughlin J, Han G, Schalper KA, Carvajal-Hausdorf D, Pelekanou V, Rehman J, et al. Quantitative assessment of the heterogeneity of PD-L1 expression in non-small-cell lung cancer. JAMA Oncol 2016;2:46–54.
18. Kerr KM, Tsao MS, Nicholson AG, Yatabe Y, Wistuba II, Hirsch FR; IASLC Pathology Committee. Programmed death-ligand 1 immunohistochemistry in lung cancer: In what state is this art? J Thorac Oncol 2015;10:985–9.
19. Hirsch FR, McElhinny A, Stanforth D, Ranger-Moore J, Jansson M, Kulangara K, et al. et al.PD-L1 immunohistochemistry assays for lung cancer: results from phase 1 of the blueprint PD-L1 IHC assay comparison project. J Thorac Oncol 2017;12:208–22.
20. Adam J, Rouquette I, Damotte D, Badoual C, Danel C, Damiola F, et al. et al. Multicentric french harmonization study for PD-L1 IHC testing in NSCLC. J Thorac Oncol 2017;12:S11–2.
21. Ratcliffe MJ, Sharpe A, Midha A, Barker C, Scott M, Scorer P, et al. Agreement between programmed cell death ligand-1 diagnostic assays across multiple

protein expression cutoffs in non–small cell lung cancer. Clin Cancer Res 2017;23:3585–91.
22. Alexandrov LB, Nik-Zainal S, Wedge DC, Aparicio SA, Behjati S, Biankin AV, et al. Signatures of mutational processes in human cancer. Nature 2013;500:415–21.
23. Schumacher TN, Schreiber RD. Neoantigens in cancer immunotherapy. Science 2015;348:69–74.
24. Taube JM, Klein A, Brahmer JR, Xu H, Pan X, Kim JH, et al. Association of PD-1, PD-1 ligands, and other features of the tumor immune microenvironment with response to anti-PD-1 therapy. Clin Cancer Res 2014;20:5064–74.
25. Zeng DQ, Yu YF, Ou QY, Li XY, Zhong RZ, Xie CM, et al. Prognostic and predictive value of tumor-infiltrating lymphocytes for clinical therapeutic research in patients with non-small cell lung cancer. Oncotarget 2016;7:13765–81.
26. Parra ER, Behrens C, Rodriguez-Canales J, Lin H, Mino B, Blando J, et al. Image analysis-based assessment of PD-L1 and tumor-associated immune cells density supports distinct intratumoral microenvironment groups in non-small cell lung carcinoma patients. Clin Cancer Res 2016;22:6278–89.
27. Schalper KA, Brown J, Carvajal-Hausdorf D, McLaughlin J, Velcheti V, Syrigos KN, et al. Objective measurement and clinical significance of TILs in non-small cell lung cancer. J Natl Cancer Inst 2015;107. pii: dju435.
28. Teng MW, Ngiow SF, Ribas A, Smyth MJ. Classifying cancers based on T-cell infiltration and PD-L1. Cancer Res 2015;75:2139–45.
29. Angell H, Galon J. From the immune contexture to the Immunoscore: the role of prognostic and predictive immune markers in cancer. Curr Opin Immunol 2013;25:261–7.
30. Edge SB, Byrd DR, Compton CC, Fritz AG, Greene FL, Trotti A. AJCC cancer staging manual. 7th ed. New York, NY: Springer; 2010.
31. Igarashi T, Teramoto K, Ishida M, Hanaoka J, Daigo Y. Scoring of PD-L1 expression intensity on pulmonary adenocarcinomas and the correlations with clinicopathological factors. ESMO Open 2016;1:e000083.
32. Salgado R, Denkert C, Demaria S, Sirtaine N, Klauschen F, Pruneri G, et al. The evaluation of tumor-infiltrating lymphocytes (TILs) in breast cancer: recommendations by an International TILs Working Group 2014. Ann Oncol 2015;26:259–71.
33. Tiseo M, Damato A, Longo L, Barbieri F, Bertolini F, Stefani A, et al. Analysis of a panel of druggable gene mutations and of ALK and PD-L1 expression in a series of thymic epithelial tumors (TETs). Lung Cancer 2017;104:24–30.
34. Eisenhauer EA, Therasse P, Bogaerts J, Schwartz LH, Sargent D, Ford R, et al. New response evaluation criteria in solid tumours: revised RECIST guideline (version 1.1). Eur J Cancer 2009;45:228–47.
35. Ansell SM, Lesokhin AM, Borrello I, Halwani A, Scott EC, Gutierrez M, et al. PD-1 blockade with nivolumab in relapsed or refractory Hodgkin's lymphoma. N Engl J Med 2015;372:311–9.
36. Gojo I, Karp JE. New strategies in acute myelogenous leukemia: leukemogenesis and personalized medicine. Clin Cancer Res 2014;20:6233–41.
37. Ghatalia P, Zibelman M, Geynisman DM, Plimack ER. Checkpoint inhibitors for the treatment of renal cell carcinoma. Curr Treat Options Oncol 2017;18:7.
38. Pilotto S, Sperduti I, Novello S, Peretti U, Milella M, Facciolo F, et al. Risk stratification model for resected squamous-cell lung cancer patients according to clinical and pathological factors. J Thorac Oncol 2015;10:1341–8.
39. Bria E, Di Modugno F, Sperduti I, Iapicca P, Visca P, Alessandrini G, et al. Prognostic impact of alternative splicing-derived hMENA isoforms in resected, node-negative, non-small-cell lung cancer. Oncotarget 2014;5:11054–63.
40. Gros A, Parkhurst MR, Tran E, Pasetto A, Robbins PF, Ilyas S, et al. Prospective identification of neoantigen-specific lymphocytes in the peripheral blood of melanoma patients. Nat Med 2016;22:433–8.
41. Huang AC, Postow MA, Orlowski RJ, Mick R, Bengsch B, Manne S, et al. T-cell invigoration to tumour burden ratio associated with anti-PD-1 response. Nature 2017;545:60–5.
42. Glanville J, Huang H, Nau A, Hatton O, Wagar LE, Rubelt F, et al. Identifying specificity groups in the T cell receptor repertoire. Nature 2017;547:94–8.
43. Ren J, Liu X, Fang C, Jiang S, June CH, Zhao Y. Multiplex genome editing to generate universal CAR T cells resistant to PD1 inhibition. Clin Cancer Res 2017;23:2255–66.
44. Ji M, Liu Y, Li Q, Li X, Ning Z, Zhao W, et al. PD-1/PD-L1 expression in non-small-cell lung cancer and its correlation with EGFR/KRAS mutations. Cancer Biol Ther 2016;17:407–13.
45. Taube JM, Anders RA, Young GD, Xu H, Sharma R, McMiller TL, et al. Colocalization of inflammatory response with B7-h1 expression in human melanocytic lesions supports an adaptive resistance mechanism of immune escape. Sci Transl Med 2012;4:127.
46. Lavin Y, Kobayashi S, Leader A, Amir ED, Elefant N, Bigenwald C, et al. Innate immune landscape in early lung adenocarcinoma by paired single-cell analyses. Cell 2017;169:750–65.
47. Langer CJ, Gadgeel SM, Borghaei H, Papadimitrakopoulou VA, Patnaik A, Powell SF, et al. Carboplatin and pemetrexed with or without pembrolizumab for advanced, non-squamous non-small-cell lung cancer: a randomised, phase 2 cohort of the open-label KEYNOTE-021 study. Lancet Oncol 2016;17:1497–508.
48. Weber JS, Kudchadkar RR, Gibney GT, De Conti RC, Yu B, Wang W, et al. Phase I/II trial of PD-1 antibody nivolumab with peptide vaccine in patients naive to or that failed ipilimumab. J Clin Oncol 2013;31:9011.
49. Alsuliman A, Colak D, Al-Harazi O, Fitwi H, Tulbah A, Al-Tweigeri T, et al. Bidirectional crosstalk between PD-L1 expression and epithelial to mesenchymal transition: significance in claudin-low breast cancer cells. Mol Cancer 2015;14:149.
50. Busch SE, Hanke ML, Kargl J, Metz HE, MacPherson D, McGarry Houghton A. Lung cancer subtypes generate unique immune responses. J Immunol 2016;197:4493–503.

Published OnlineFirst October 26, 2017; DOI: 10.1158/1078-0432.CCR-17-2156

Clinical Cancer Research

Low PD-1 Expression in Cytotoxic CD8$^+$ Tumor-Infiltrating Lymphocytes Confers an Immune-Privileged Tissue Microenvironment in NSCLC with a Prognostic and Predictive Value

Giulia Mazzaschi, Denise Madeddu, Angela Falco, et al.

Clin Cancer Res 2018;24:407-419. Published OnlineFirst October 26, 2017.